

CFD Simulations of a Co-current Spray Dryer

Saad Nahi Saleh

Abstract—This paper presents the prediction of air flow, humidity and temperature patterns in a co-current pilot plant spray dryer fitted with a pressure nozzle using a three dimensional model. The modelling was done with a Computational Fluid Dynamic package (Fluent 6.3), in which the gas phase is modelled as continuum using the Euler approach and the droplet/ particle phase is modelled by the Discrete Phase model (Lagrange approach). Good agreement was obtained with published experimental data where the CFD simulation correctly predicts a fast downward central flowing core and slow recirculation zones near the walls. In this work, the effects of the air flow pattern on droplets trajectories, residence time distribution of droplets and deposition of the droplets on the wall also were investigated where atomizing of maltodextrin solution was used.

Keywords—Spray, CFD, multiphase, drying, droplet, particle.

I. INTRODUCTION

SPRAY dryer is an essential unit operation for the manufacture of many products with specific powder properties, e.g. chemical, ceramic, food; pharmaceuticals etc.

In spite of the wide uses of the spray dryers, they are still designed mainly on the basis of experience and pilot experiment [1]. One of the big problems facing spray dryer designer and operators is the complexity of the spray/air mixing process in spray chamber [2] where the air flow patterns existing inside the spray dryer is considered as one of the primary factors that influence the residence time of droplet / particle, in turn the equality of the product produced by the dryer such as moisture content, size distribution, and bulk density. The particle residence time and surrounding air temperature are particularly important in the spray drying of thermal sensitive products, such as milk, where product degradation can occur if the particles remain in an air stream for too long, or experience an air stream is too hot [3].

A very important phenomenon of spray dryer operability is the particle wall deposition which is affected by the temperature and humidity patterns inside the dryer when moist particles contact the spray dryer wall. Such depositions can lead to a build up large amounts of product on the wall. These depositions may be dangerous, as they can fall and cause damage to the chamber walls, or they can char, resulting in a potential explosion hazard [4]. Application of computational fluid dynamic (CFD) techniques in analyses of spray dryers have been carried out successfully and reported by [5], [6] and others. Most of these earlier works assume the flows in the dryers are two-

dimensional and axisymmetric in order to reduce the demand on computational resources. There is clear experimental evidence to demonstrate three dimensional behavior in this type of equipment suggesting that numerical simulations of spray dryers need to include the three-dimensional nature of the flows [7]. Previous two-dimensional, axisymmetric simulations can only be regarded as indicative, at best, since they do not reproduce the basic physics that are involved [8].

As explained above, it is apparent that in order to avoid wall build up and insufficient residence time of particle which influences the product quality, we must able to model of the complexity of the spray/air mixing and including the proper drying model, therefore the objective of this paper is to perform two phase simulations of a co-current spray dryer in order to examine what current computational fluid dynamics techniques are capable of achieving when simulating such a system and to understand what happened inside the spray dryer?

II. MODELLING APPROACH

In order to simulate the spray drying process in a rigorous way, it is necessary to gain insight into the flow pattern, local temperature and local moisture content of the air and the temperature-time history of drying particle.

The first important aspect in modelling of spray dryer is prediction of the flow pattern of air which depends on the geometry of the dryer and the location and design of the air inlet and air outlet channel. The trajectories followed by the drying particles depend not only on the air flow pattern but also on the position and method of atomization.

The second important aspect is the need to include the proper modelling of the drying behaviour of the droplet to ensure that the prediction of the droplet behaviour in the dryer is correct. The above considerations will be discussed in more detail as follows.

A. Two Phase Flow Simulation

The flow in a spray dryer is turbulent and two-phase (gas and droplets or gas and particles). There are two commonly used approaches for modelling two-phase flow[9]. Firstly, one can treat the disperse phase as an extra fluid with its own flow field (Euler/Euler approach). In the case of spray drying, with rather concentration of particles, one usually use the second approach, the Euler/ Lagrange approach. In this approach the gas field is calculated first (Euler). This is done by calculating solutions of the Navier-Stokes and continuity equation on a grid of control volumes. Subsequently the particles are tracked individually (Lagrange). Along the particle trajectories the exchange of mass, energy and

Saad Nahi Saleh is with the Chem. Eng. Dept., Tikrit University, Iraq (e-mail: saad_nahi68@yahoo.com).

momentum with the continuous phase is calculated. These transfer terms are added to the source terms of the Navier-Stokes equations of the gas flow calculation. After the particle tracking, the air flow calculation pattern is recalculated, taking the transfer terms into account. This cycle of airflow calculation followed by particle tracking is repeated until convergence is reached. This scheme is called the Particle-In-Cell model [10].

The droplet field is established by integrating the differential equations for droplet motion to determine droplet velocities and, with further integration, droplet trajectories. At each time step along the trajectory, droplet size and temperature history are calculated using the equations for droplet mass and heat transfer rates. These equations can be found in [11]. Since space is limited, they are not repeated here.

The effect of turbulence on the droplet motion is modelled by the turbulent stochastic model. Turbulent stochastic tracking of droplets admits the effect of random velocity fluctuations of turbulence on droplet dispersion to be accounted for in prediction of droplet trajectories [12].

B. Droplet Drying

In this modelling approach, the drying kinetics are included and the concept of a characteristic drying curve has been used here [13]. This essentially empirical approach has been widely used for the modelling of single particle drying, where it was based on the assumption of two distinct periods of drying, namely, the constant rate period which is then followed by the falling rate period. The approach relies upon first identifying an unhindered drying rate which may correspond to the rate in the first/constant drying period, and may mathematically expressed as

$$\hat{N} = \frac{dm}{dt} = k_c A_d M_w (C_{w,s} - C_{w,\infty}) \quad (1)$$

The relative drying rate, ξ , is then defined

$$\xi = \frac{N}{\hat{N}} \quad (2)$$

Where N is the drying rate and \hat{N} is the unhindered drying rate. ξ is a function of the characteristic moisture content, defined as

$$\xi = f(\Phi) \quad \text{if} \quad x \leq x_{cr} \\ \xi = 1 \quad \text{if} \quad x > x_{cr} \quad (3)$$

$$\Phi = \frac{x - x_{eq}}{x_{cr} - x_{eq}}$$

The drying curve can be fitted by a simple expression of the form [14]:

$$\xi = \frac{N}{\hat{N}} = \Phi^n = \left(\frac{x - x_{eq}}{x_{cr} - x_{eq}} \right)^n \quad (4)$$

According to [15], the value of n for maltodextrin is 3.22.

Where x is the volume-averaged moisture content, x_{cr} is the critical moisture content and x_{eq} is the solid moisture content

which would be in equilibrium with the surrounding gas and can be predicted from correlation of sorption isotherms of the dried material such as the one proposed by [16].

$$x_{eq} = \frac{1}{100} \left[\frac{\ln(1-\psi)}{-c_1(T+c_2)} \right]^{1/m} \quad (5)$$

Where x_{eq} is the equilibrium moisture content on a dry basis (in kg water/kg dry material), T is the temperature of the gas (in K), and ψ is the relative humidity of the gas (a fraction from 0 to 1), and c_1 , c_2 and m are constants with the values 0.000405, -187.962 and 1.169 respectively.

The characteristic drying curve for a given material is unique and independent of external drying conditions. Furthermore, it is hypothesized that the drying-rate curves for the same material at different operating conditions will be geometrically similar, *i.e.*, the normalized drying rate curve characterizes the drying of a given material [17], therefore it can be assumed that the critical moisture content is the same as the initial moisture content.

The concentration of vapour at the droplet surface is evaluated by Raoult's Law, where the partial pressure of the vapour at the surface is equal to mole fraction of the water (X_s) multiplied by the saturated vapour pressure, P_{sat} at the droplet temperature, T_d :

$$C_{w,s} = \frac{X_s P_{sat}}{RT_d} \quad (6)$$

The concentration of vapour in the bulk gas is calculated by:

$$C_{w,\infty} = Y_{w,\infty} \frac{P}{RT_\infty} \quad (7)$$

Where $Y_{w,\infty}$ is the local bulk mole fraction of water vapour,

P is the local absolute pressure, and T_∞ is the local bulk temperature in the gas. The mass transfer coefficient in (1) is calculated from the Sherwood number correlation [18]:

$$Sh_{AB} = \frac{k_c d_d}{D_{i,m}} = 2.0 + 0.6 Re_d^{1/2} Sc^{1/3} \quad (8)$$

III. CASE STUDY

For CFD simulation, the spray dryer used in this article is a co-current pilot plant spray dryer by Niro Atomizer as shown in Fig. 1. The geometry and air inlet size are the same as those used by [6]. The nozzle atomizer is located at the top of the drying chamber; hot drying air enters the chamber through an annulus with the nozzle as its centre. The outlet of the spray dryer is a pipe mounted through the wall of the cone section of the chamber, bent downwards in the centre of the chamber.

This type of spray dryers is a more complex geometry than the simple box configuration, which requires an unstructured mesh for accurate representation using 84000 tetrahedral mesh elements (Fig. 2). To check whether the solution was dependent on the mesh which had chosen, the mesh was refined to 160000 elements. For each element of original

mesh, the value of axial, radial and tangential velocities was compared with the corresponding values in refined mesh.

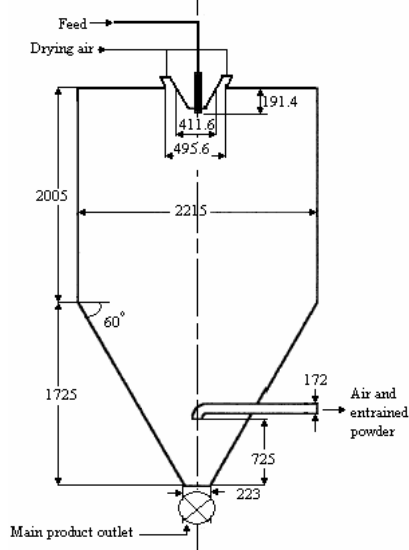


Fig. 1 The geometry of the pilot plant spray dryer (the dimensions in mm)

The differences were smaller than 4%, therefore we can say that solution is mesh independence. As a first step, the modelling of the air flow without spray and swirl is performed. A second step will be the modeling the temperature and humidity when pure water droplets are tracked through the air under operational conditions with 5 swirl degree.

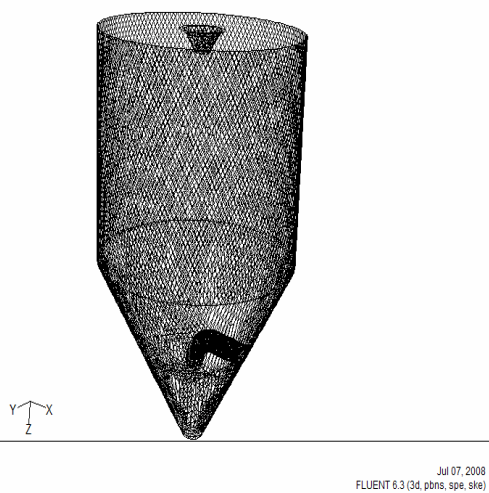


Fig. 2 Surface mesh for the pilot plant spray dryer

The last stage is modeling the spray drying process of maltodextrin solution in co current spray dryer. For modelling the air flow without spray, the velocity components (axial, radial and tangential) of inlet air were: 6.03, -4.22 and 0.0 m/s respectively. Two feed are used for simulating, 42 kg/hr of

pure feed water and 50 kg/hr of 42.5 wt% maltodextrin solution. The nozzle was a hollow-cone-type centrifugal pressure nozzle (Spraying Systems Co.: SX-type), spray angle and velocity for pure water are 73° and 49 (m/s) respectively while for maltodextrin solution are 76° and 59 (m/s) . A spray is represented by a 10 droplet sizes, ranging from 10 to $138 \mu\text{m}$. Rosin Rammler distribution parameters (mean diameter and power) are ($68.6 \mu\text{m}$ and 2.45) for pure water ($70.5 \mu\text{m}$ and 2.09) for maltodextrin solution.

IV. BOUNDARY CONDITIONS

A $k-\varepsilon$ model was chosen to model the turbulence. The $k-\varepsilon$ model is the most commonly used in engineering practice because it convergence considerably better than the algebraic stress model (ASM) and Reynolds stress model (RSM) and require less computational effort [6]. To determine the fate of the droplet trajectory when hit the wall of the drying chamber, Fluent [11] submit multi options that could selected for the present work. The possible fates for a droplet trajectory are as "escaped", "trapped", "evaporated", "reflected" and "coalesced". In this work, 100 droplet trajectories were calculated and the "escaped" boundary condition is used, where the droplets are lost from calculation at the point of impact with the wall. Of each droplet trajectory, the time of flight and the location of the end-point were calculated. In order to compare the CFD predicted results with experimental results of [6], the same conditions were used as tabulated in Table 1.

V. RESULTS AND DISCUSSION

Analysis of the CFD simulation of air velocity profile without spray in the spray dryer, as shown the contour of air velocity (Fig. 3), showed that the flow field consists of a fast flowing downward core with a slow recirculation around that core near the upper section of the conical part of the chamber. The core broadens as going down to the outlet. The predicted and measured velocities at different levels are depicted in Fig. 4. One note that the central core is of the radius of about 0.25 m and the reminder of the chamber is at very low velocity (0.2 m/s). The highest velocity magnitude in the core is about 6.75 m/s at the 0.6 m level. The sharp descent of velocity magnitude at the axis of the chamber is reduced as the air goes into the cone section of the chamber. This trend is agreed very well with the measured results. Only the predictions of velocity magnitudes at 1.0 m level are somewhat higher than the measured values. We expect the reason is that the air flow reveals periodicity in the velocity magnitude at several locations in the chamber and the 1.0 m level is one of its. This nature of air flow was noticed by [6] when measuring the velocity signal in these locations. Therefore we can say that the air flow in this pilot plant spray

dryer is transient in nature and we need a transient CFD simulation to consider this behaviour.

TABLE I
BOUNDARY CONDITIONS USED FOR CASE STUDY

Air flowrate (m^3/s)	Air temp. ($^{\circ}C$)	Air humidity (kg_w/kg_a)	Feed temp. ($^{\circ}C$)
0.42	195	0.009	27
Air axial velocity (m/s)	Air radial velocity (m/s)	Air tangential velocity (m/s)	Swirl Degree
7.42	-5.19	0.649	5
Pressure at outlet (Pa)	Turb. - k - value (m^2/s^2)	Turb. - ε - value (m^2/s^3)	Chamber wall thickness (m)
-150	0.027	0.37	0.002
Wall material	Wall heat transfer coefficient ($W/m^2.K$)	Air temp. outside wall ($^{\circ}C$)	Wall boundary condition
Steel	3.5	25	escaped

It is important to mentioned that the air flow pattern for the feed water and maltodextrin look very similar to the air flow with no spray (Fig. 3), and this emphasize that effects of droplet/ particles on the air flow pattern in the spray dryer is very weak, therefore we can adopted the hypothesis which ignoring the effects of droplets on the gas flow pattern if the feed rate is less than 10% of the gas mass flow rate [19], [20].

In Fig. 5 and 6, the predicted counters of temperature and humidity of air with maltodextrin spray are depicted. From these figures, it can seen that a large volume of the chamber has almost constant temperature and humidity ($120^{\circ}C$, $0.032 kg_w/kg_a$). It appears that most of the evaporation takes place in the fast flowing core.

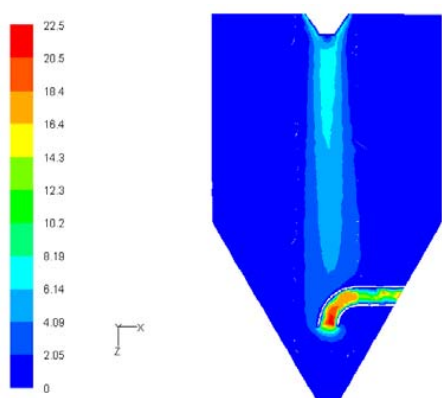


Fig. 3 Contour of predicted air velocity (m/s) in the spray dryer chamber (without spray)

It is practical to compare the predicted values with the measured values at certain points like outlet. As shown in Fig. 5 and 6, the predicted values of temperature and humidity for maltodextrin solution spray at outlet are $115^{\circ}C$ and $0.033 kg_w/kg_a$ and this agreed well with measured temperature and humidity at the outlet (the measured values at outlet are $113^{\circ}C$ and $0.031 kg_w/kg_a$). The predicted values of temperature and humidity for water spray at outlet are $88^{\circ}C$ and $0.044 kg_w/kg_a$, and this agreed well with measured temperature and humidity at the outlet (the measured values at outlet are $86^{\circ}C$ and $0.043 kg_w/kg_a$).

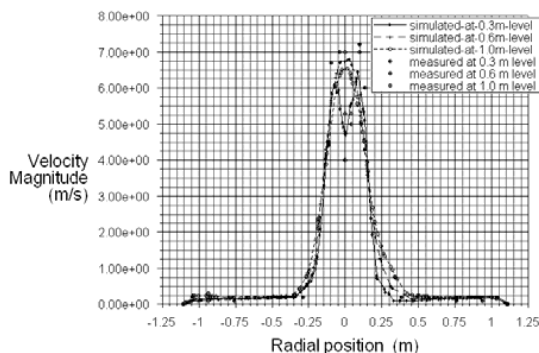


Fig. 4 Predicted and measured velocities at different levels measured from the ceiling (0.3, 0.6, 1.0 m) in the spray drying chamber

In Fig. 7, a 100 particle trajectories which represent the spray of 10 particle sizes are predicted. It is clearly seen that the particles have different fates and different flight times (particle residence time). As can be seen, a bigger particles (greater than $81 \mu m$) appear to be able to penetrate the fast flowing core into the slow recirculation zone whereas the smaller particles are trapped in this core where the massive evaporation occur for this smaller droplets/ particles in the core region due to high air temperature as shown in contour of temperature pattern (Fig. 5), therefore the bigger particles have longer residence time than the smaller particle (the mean residence time of $138 \mu m$ particle is 3.6 second while is 1.85 second for $10 \mu m$ particle), and this is opposite to what estimated by previous models such as Kerkhof's model [21] which was based upon gravity effect and neglect the air flow pattern behaviour inside the spray dryer.

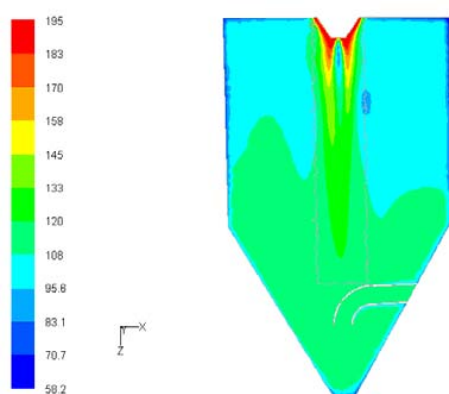


Fig. 5 Contour of predicted air temperatures ($^{\circ}\text{C}$) distribution in the spray dryer (with maltodextrin spray)

It is generally assumed that the residence time distributions of the particles/droplets are equal to those of the air (Masters (14)). With air flow rate $0.421 \text{ m}^3/\text{s}$, a mean residence time of air is (24.2 s) in this dryer [6]. Analysis of CFD simulation shows that mean particles residence time in the dryer (2.4 s) is shorter than mean air residence time.

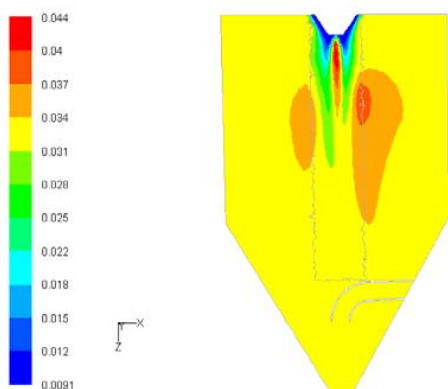


Fig. 6 Contour of predicted air humidities (kg_w/kg_a) distribution in the spray dryer (with maltodextrin spray)

It is found that a large fraction of the droplets (45%) hit the conical part of the chamber wall, 9% of the droplets hit the cylindrical part of the chamber wall, 25% hit the outside of the air outlet, 1% of the particles hit the roof and 20% of particles were dragged along to the cyclone. It is expected that this large deposition at the conical part is because of the air flow pattern effects in this region where the air approaches the wall at right angles, the air velocity is zero, and this location can be considered as stagnation point (Fig. 8) which reveal higher deposition. This explanation is consistent with the measured results [22].

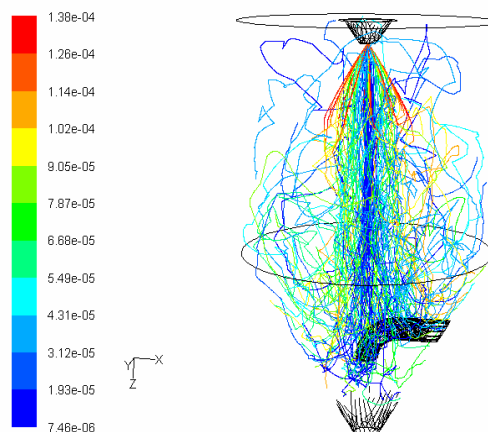


Fig. 7 Predicted droplet trajectories (100 droplet tracks represent a 10 droplet size distribution) in the spray dryer chamber. The colour of each trajectory indicate the size of droplet (in m) as shown in the left column.

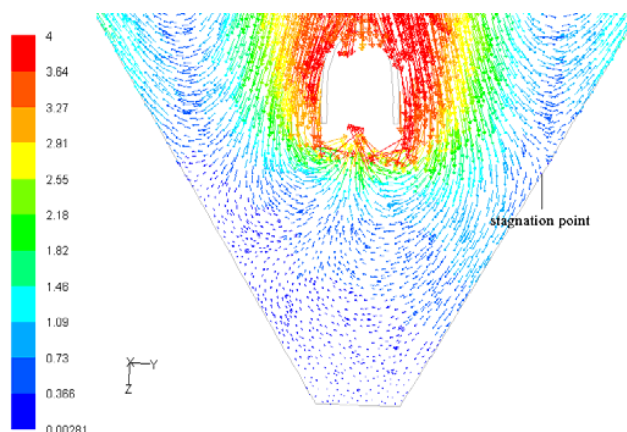


Fig. 8 Vector plot of the predicted air velocity (m/s) in the lower conical of the spray dryer chamber.

VI. CONCLUSION

The CFD simulations correctly predict the internal behaviour of the spray dryer. It discerned that the air flow at specified conditions consist of fast flowing core and slow recirculation zone around it, and the air flow reveals a periodicity in some locations in the dryer which can simulated by a transient CFD model. The drying of droplet take place in the core region where the smaller droplets evaporated due to high air temperature. The air flow pattern have an important effect upon the trajectories of the particles

that specify the particle history and its fate inside the spray dryer, and in turn, the air flow pattern play an important role in existence of the deposition and in the quality of the product, in addition to the performance of the spray dryer.

The air flow pattern with water or maltodextrin solution spray is very similar to that without spray, therefore the effect of particles on the air flow can be neglected in the spray dryer.

NOMENCLATURE

A_d	droplet surface area	m^2
$C_{w,s}$	concentration of vapour	$kmol/m^3$
$D_{w,m}$	diffusion coefficient	m^2/s
d_d	droplet diameter	μm
k_c	mass transfer coefficient	m/s
M_w	molecular weight of vapour	$kg/kmol$
m	droplet mass	kg
N	drying rate	kg/s
P	pressure	pa
R	universal gas constant	$(J/K \cdot mol)$
T	temperature	K
t	time	s
Re	Reynolds number	-
Sc	Schmidt number	-
Sh	Sherwood number	-
x	moisture content	kg_w/kg_s
X	mole fraction in liquid	-
Y	mole fraction in gas	-
Greek letters		
ξ	relative drying rate	-
Φ	characteristic moisture content	-
ψ	relative humidity	-
subscript		
cr	critical	
eq	equilibrium	
d	droplet	
s	droplet surface	
sat	saturation	
w	water	
∞	bulk air	

REFERENCES

- [1] Masters, K., *Spray Drying Handbook*, 4th ed., John Wiley and Sons, New York, 1985.
- [2] Oakley, D.E., Produce uniform particles by spray drying, *Chem. Eng. Prog.*, October, pp. 48-54, 1997.
- [3] Harvie, D.J.E.; Langrish, T.A.G.; Fletcher, D.F., A computational fluid dynamics study of a tall-form spray dryer, *Trans. IChemE*, 80(3), pp. 163-175, 2002.
- [4] Harvie, D.J.E.; Langrish, T.A.G.; Fletcher, D.F., Numerical simulations of gas flow patterns within a tall-form spray dryer, *Trans. IChemE*, 79(3) A, pp. 235-248, 2001.
- [5] Oakley, D.E.; Bahu, R.E., Computational modeling of spray drying, *Comput. Chem. Eng.* 17, pp. 493-498, 1993.
- [6] Kieviet, F.G., *Modelling Quality in Spray Drying*, Ph.D. thesis, Eindhoven University of Technology, the Netherlands, 1997.
- [7] Southwell, D.B.; Langrish, T.A.G., Observations of flow patterns in a spray dryer, *Drying Technology*, 18(3), pp. 661-685, 2000.
- [8] Langrish, T.A.G.; Fletcher, D.F., Prospects for the Modelling and Design of Spray Dryers in the 21st Century, *Drying Technology*, 21(2), pp. 197-215, 2003.
- [9] Sommerfeld, M., Review on numerical modeling of dispersed two phase flows, *Proc. 5th Int. Symp. on Refined Flow Modelling and Turbulence Measurements*, Paris, 1993.
- [10] Crowe, C.T.; Sharma, M.P.; Stock, D.E. The particle-source-in-cell (PSI-Cell) model for gas-droplet flows, *Journal of Fluid Engineering*, 99, pp. 325-332, 1977.
- [11] Fluent Manual, Chap. 23: Discrete phase models, www.fluent.com, 2006.
- [12] Haung, L.; Kumar, K.; Mujumdar, A. S., A Parametric Study of the Gas Flow Patterns and Drying Performance Of Co-current Spray Dryer, *Drying Technology*, 21, 6, pp. 957-978, 2003.
- [13] Langrish, T.A.G.; Kockel, T.K., The implementation of a characteristic drying curve for milk powder using a computational fluid dynamics simulation, *Chem. Eng. J.*, 83(4), pp. 69-74, 2001.
- [14] Keey, R., *Drying of Loose and Particulate Matter*, 1st edn, Hemisphere Publishing Corporation, 1992.
- [15] Woo, M.W.; Daud, W.R.; Mujumdar, A.S.; Talib, M.Z.; Hua, W.Z. and Tarsiran, S. M., Comparative study of droplet drying models for CFD modeling, *Chem. Eng. Res. and Des.*, 86, pp. 1038-1048, 2008.
- [16] Truong, V.; Bhandari, B.R.; Howes, T., Optimization of co-current spray drying process of sugar-rich foods. Part I—moisture and glass transition temperature profile during drying, *Journal of Food Engineering* 71(1), pp. 55-65, 2005.
- [17] Handscomb, C., Kraft, M., Bayly, A., *Spray Drying Modelling*, University of Cambridge, 2005.
- [18] Ranz, W.; Marshall, W., Evaporation from drops, *Chem. Eng. Prog.*, 48(141), pp. 173, 1952.
- [19] Reay, D., Modelling continuous convection dryers for particulate solids—progress and problems, *Drying '85*, 5, pp. 67-74, 1985.
- [20] Elghobashi, S., On predicting particle-laden turbulent flows, *Applied Scientific Research*, 52, pp. 309-329, 1994.
- [21] Kerkhof, P.J.A.M.; Schoeber, W.J.A.H., Theoretical modeling of the drying behaviour of droplet in spray dryers, *Advances in preconcentration and dehydration of foods*, ed. A. Spicer, Applied science publisher, London, pp. 349-397, 1974.
- [22] Kota, K.; Langrish, T., Prediction of Deposition Patterns in a Pilot-Scale Spray Dryer Using CFD Simulations, *Chem. Prod. and Proc. Modeling*, 2(3), 26, 2007.